GRM 2023 – Fourth International Workshop on Gravitomagnetism and large-scale rotation measurement, 14 -16 June 2023 (W-F),Pisa

Astrodynamical Missions, Gravitomagnetism, and the Astronomical Reference frames

Wei-Tou Ni

Wuhan Institute of Physics and Mathematics, APM, CAS

Refs (listed in 3rd GRM) (i) Ciufolini & Wheeler, Grav. & Inertia (1995); Ciufolini et al., *Eur. Phys. J. C* 79:872 (2019)

(ii) A Gebauer, M Tercjak, K U Schreiber et al., *Phys. Rev. Lett*. 125:033605 (2020);

(iii) A Di Virgilio, et al., Underground Sagnac gyroscope with sub-prad/s … sensitivity *Phys. Rev. Res.* 2 032069(R) (2020);

(iv) Z Li, K Liu, …, J. Zhang, Proposal … in large-scale passive resonant gyroscopes, *Opt. Express* 7,9737 (2021)

(v) C Schubert, …, E M Rasel; Muti-loop atomic Sagnac interferometry, *Scientific Report* 11, 16121 (2021);

(vi) Z-W Yao, …, R-B Li et al., Self-alignment of a … dual-AI gyro …, *Phys. Rev. A* 103, 023319 (2021);

(vii) Y Li,…, Z Li, Thermal phase noise in giant interferometric fiber optic gyroscopes, Opt. Express 27, 14121 (2019)

(viii) W-J Xu, … M-K Zhou, Z-K Hu, … tilt and … a sensitive AI gyroscope, Opt. Express 28, 12189 (2019)

(ix) T-y Huang, Astrodynamics in ASTROD I, Publication of PMO 23, 21 (2004);

(x) IERS Conventions, G. Petit and Brian Luzum, eds.IERS Technical Note No. 36 (2010)

GRM 2021 – Third International Workshop on Gravitomagnetism and large-scale rotation measurement, November 25-26, 2021 Wuhan, China

Gravitomagnetism, rotation measurement and the astronomical reference frame

Wei-Tou Ni

Wuhan Institute of Physics and Mathematics, APM, CAS

Refs (i) Ciufolini & Wheeler, Grav. & Inertia (1995); Ciufolini et al., *Eur. Phys. J. C* 79:872 (2019)

(ii) A Gebauer, M Tercjak, K U Schreiber et al., *Phys. Rev. Lett*. 125:033605 (2020);

(iii) A Di Virgilio, et al., Underground Sagnac gyroscope with sub-prad/s … sensitivity *Phys. Rev. Res*. 2 032069(R) (2020);

(iv) Z Li, K Liu, …, J. Zhang, Proposal … in large-scale passive resonant gyroscopes, *Opt. Express* 7,9737 (2021)

(v) C Schubert, …, E M Rasel; Muti-loop atomic Sagnac interferometry, *Scientific Report* 11, 16121 (2021);

(vi) Z-W Yao, …, R-B Li et al., Self-alignment of a … dual-AI gyro …, *Phys. Rev. A* 103, 023319 (2021);

(vii) Y Li,…, Z Li, Thermal phase noise in giant interferometric fiber optic gyroscopes, Opt. Express 27, 14121 (2019)

(viii) W-J Xu, … M-K Zhou, Z-K Hu, … tilt and … a sensitive AI gyroscope, Opt. Express 28, 12189 (2019)

(ix) T-y Huang, Astrodynamics in ASTROD I, Publication of PMO 23, 21 (2004);

(x) IERS Conventions, G. Petit and Brian Luzum, eds.IERS Technical Note No. 36 (2010)

talks before my talk in this workshop makes the introduction of my talk easier

- Gravitomagnetic field and gravitational waves, by Matteo Luca Ruggiero (Università degli Studi di Torino)
- Large scale space interferometry to measure galactic gravitomagnetism, Angelo Tartaglia (Politecnico di Torino), Massimo Bassan (Istituto Nazionale di Fisica Nucleare)

Sagnac Effect (1913) & Lense-Thirring (1918

Local Inertial frame
No rotation
No acceleration

- EEP → Local Physics is special relativity
- A local Minkowski frame is a local inertial frame characterized by lack of inertial effects (e.g., lack of Sagnac effect when strapped down in local inertial frame).

  Units and metrology as defined by SI in local inertial frame is universal by EEP and the quantum principle (quantum metrology)
- Lense-Thirring effect can not be observed locally, i.e., can only be observed by comparison in different locations (e.g., on Earth) and/or to a distance object/observer (e.g., a quasar)

Local Inertial frame

§(2): *English Translation of the Thirring–Lense Papers*

1918 On the Effect of Rotating Distant Masses in Einstein's Theory of Gravitation

HANS THIRRING

1918 On the Influence of the Proper Rotation of Central Bodies on the Motions of Planets and Moons According to Einstein's Theory of Gravitation

J. LENSE and H. THIRRING

1984 Translation

On the Gravitational Effects of Rotating Masses: The Thirring–Lense Papers[1]

BAHRAM MASHHOON, FRIEDRICH W. HEHL, and DIETMAR S. THEISS

Institut für Theoretische Physik, Universität zu Köln, D-5000 Cologne 41, Federal Republic of Germany

Einstein Equation and Lense-Thirring Frame Dragging

$A_{\mu,\beta}{}^{\beta} = 4\pi J_{\mu}$,

with gauge condition

$A_{\alpha,}{}^{\alpha} = 0.$

The retarded solution of equation (12) is

$A_{\mu} = \int (J_{\mu}/r)_{\text{retarded}}\,(d^3x')$.

$G_{\mu\nu} = \kappa\, T_{\mu\nu}$,

$R_{\mu\nu} = 8\pi G_N\,[T_{\mu\nu} - (1/2)(g_{\mu\nu}T)]$

$h_{\mu\nu,\beta}{}^{\beta} = -16\pi G_N[T_{\mu\nu} - (1/2)(\eta_{\mu\nu}T)] + O(h^2)$

$h_{\mu\nu} = -[(4G_N)/(c^4)] \int \{[T_{\mu\nu} - (1/2)\, g_{\mu\nu}T]/r\}_{\text{retarded}}\,(d^3x') + O(h^2)$

In harmonic gauge

- For weak Field, $g_{\mu\nu} = \eta_{\mu\nu} + h_{\mu\nu}$; $U \sim h_{00}$, $A^{(g)}{}_i \sim h_{0i}$, $B^{(g)}{}_i \sim \varepsilon_{ijk} \nabla_j h_{0k}$
- *For stationary solution, no need for "retarded"*
- *For rotaing body, mass movement* → $T_{0i} \neq 0$ → $h_{0i} \neq 0$
- $h_{0i} \sim$ *Newtonian potential/*$c^2 \times \Omega \sim$ *(for Earth)* $10^{-9}\,\Omega_{earth}$; $\Omega_{earth} = 7.3 \times 10^{-5}$ **rad/sec**

Torque on Gyroscope & Effect on Laser Ring Gyro

- In general relativity, the torque on gyroscope with angular momentum ***S*** in weak field and slow-motion approximation is

  $\boldsymbol{\tau} \cong (1/2)\boldsymbol{S} \times \boldsymbol{H} = (d\boldsymbol{S}/dt) \equiv \Omega\text{-dot} \times \boldsymbol{S}.$
- $\Omega\text{-dot} = -(1/2)\boldsymbol{H} = [-\boldsymbol{J}(\boldsymbol{x} \cdot \boldsymbol{x}) + 3(\boldsymbol{J} \cdot \boldsymbol{x})\boldsymbol{x}]/|\boldsymbol{x}|^5$
- Precession of satellite orbits
- On Earth, the rotation rate depends on latitudes and would be measured at different latitude locations to better extract the Lense-Thirring effect and to form a reference system

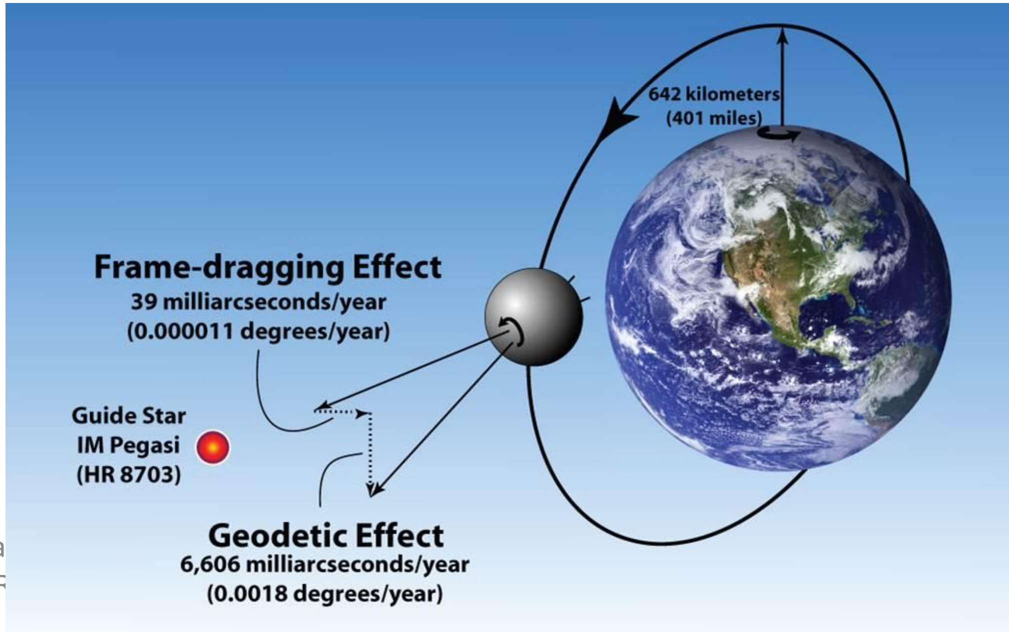

Gravity Probe B

2004 launch (19%)

Earth rotation rate
7.3×10^{-5} rad/s

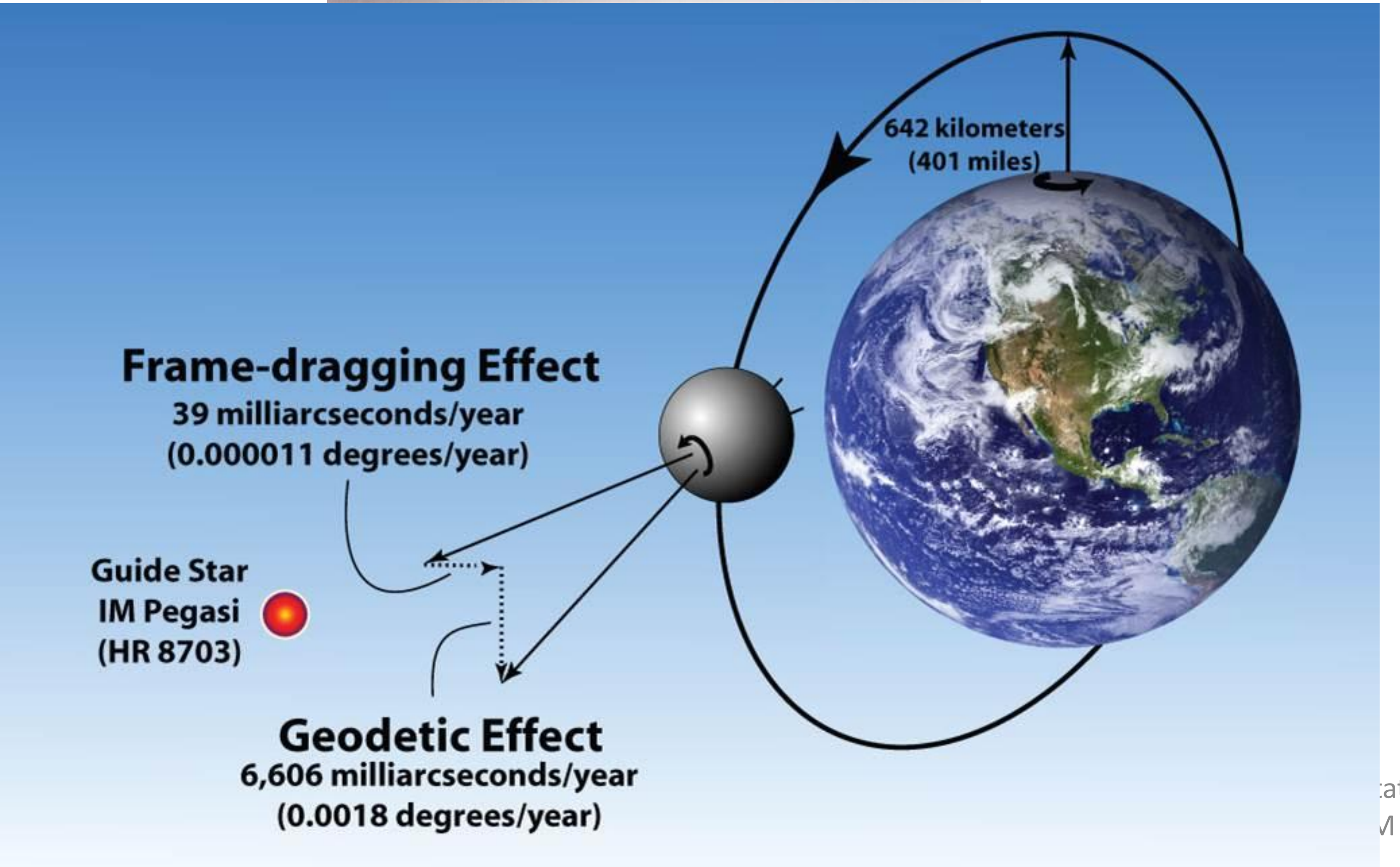

1st GRM → now

Lense-Thirring measurement from LAGEOS and LARES satellites

Ciufolini et al.

- $\mu = (0.994 \pm 0.002)$

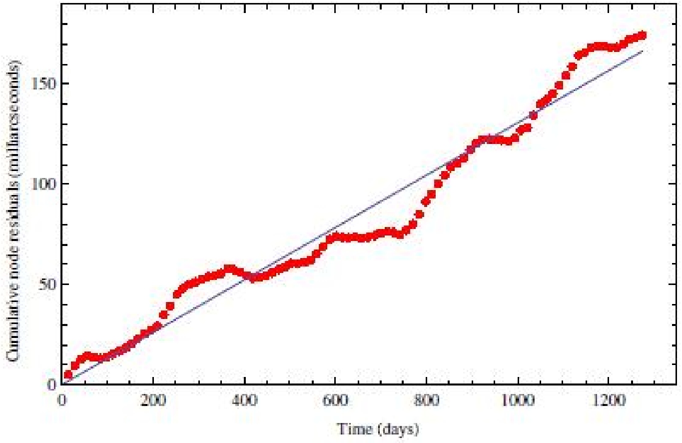

Fig. 3 Fit of the cumulative combined nodal residuals of LARES, LAGEOS, and LAGEOS 2 with a linear regression only

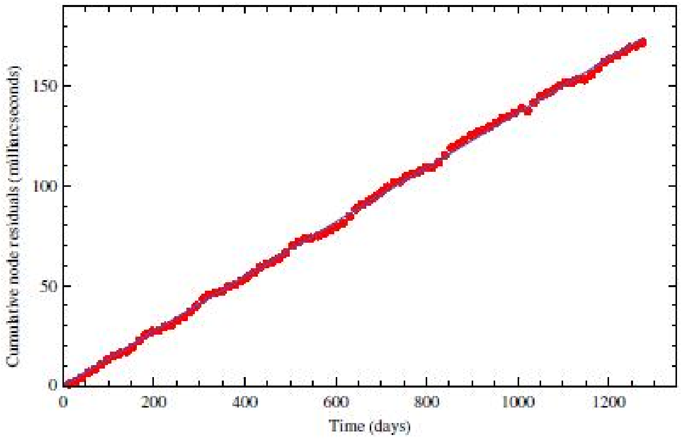

Fig. 4 Fit of the cumulative combined nodal residuals of LARES, LAGEOS, and LAGEOS 2 with a linear regression plus six periodical terms corresponding to six main tidal perturbations observed in the orbital residuals

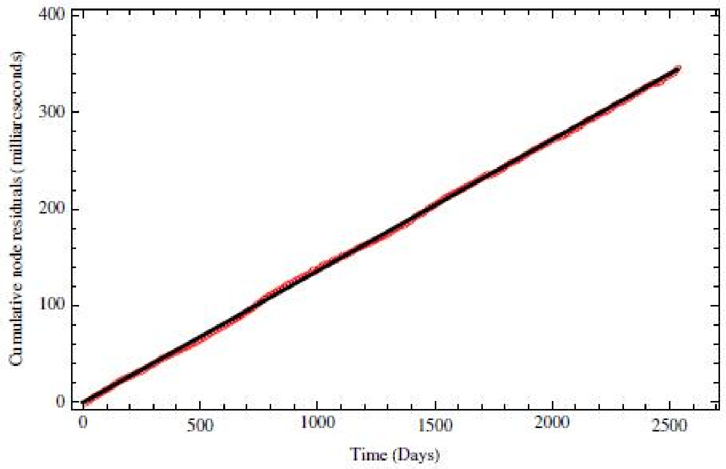

Fig. 1 Cumulative combined residuals of LARES, LAGEOS and LAGEOS 2 (shown in red), over about 7 years of orbital observations, after the removal the five main residual tidal signals. The solid black line is the fitted secular trend. The formal error of the fit is less than 0.001

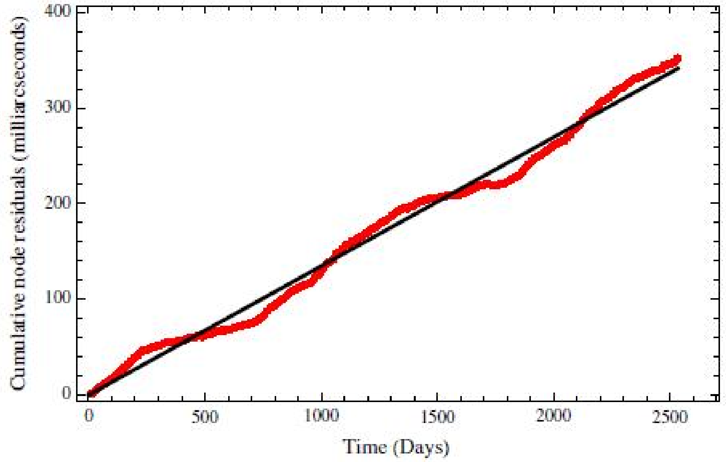

Fig. 2 Cumulative combined residuals of LARES, LAGEOS and LAGEOS 2 (shown in red), over about 7 years of orbital observations, fitted with a constant trend (shown with a solid black line)

Eur. Phys. J. C (2016) 76:120
DOI 10.1140/epjc/s10052-016-3961-8

THE EUROPEAN PHYSICAL JOURNAL C

CrossMark

Regular Article - Theoretical Physics

A test of general relativity using the LARES and LAGEOS satellites and a GRACE Earth gravity model

Measurement of Earth's dragging of inertial frames

Ignazio Ciufolini[1,2,a], Antonio Paolozzi[2,3], Erricos C. Pavlis[4], Rolf Koenig[5], John Ries[6], Vahe Gurzadyan[7], Richard Matzner[8], Roger Penrose[9], Giampiero Sindoni[10], Claudio Paris[2,3], Harutyun Khachatryan[7], Sergey Mirzoyan[7]

LARES 2

- A second satellite, LARES 2,
  launched on 13 July 2022
  with end of life date March 2062
- 297.5 kg, radius 212 mm
- LARES-2 is a sphere 36.4 cm diameter and
  a density of 15.3 g/cm^3. 303 corner cubes
- Altitude: 5899 km
- LARES 2 may improve the accuracy of the Earth frame-dragging effect measurement to 0.2%.

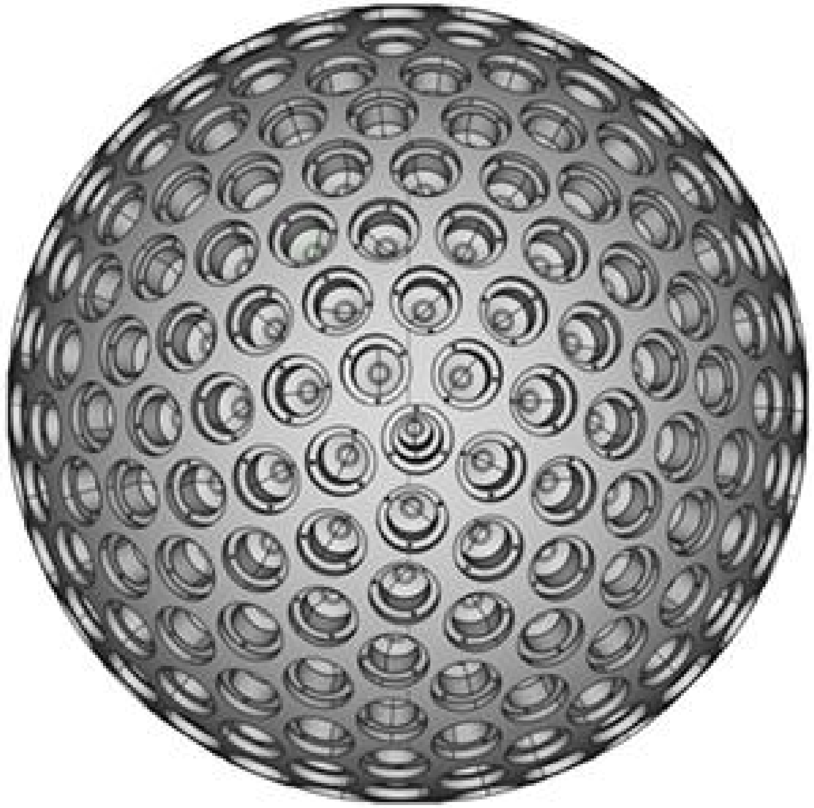

Astrodynamical Missions, Gravitomagnetism and Reference Frames

- Frame dragging is a crucial aspect of relativistic gravity and a manifestation of gravitomagnetism. It is important in the binary spin interaction of compact objects
- After Lense-Thirring papers, over 100 years of theoretical investigation and experimental endeavor have established the precision in the astrodynamical measurement up to 1 % level by Gravity Probe B and LAGEOS-LARES mission.
- Planned/Proposed astrodynamical missions, e.g. ASTROD, ASTROD-GW, LISA, LISAmax, Super-ASTROD, etc. will measure and separate the gravitomagnetic effects from their other goals. This will further improve the precision of measuring gravitomagnetic effects experimentally.
- Ongoing large-scale rotation experiments on earth and underground are reaching the sensitivity of measuring gravitomagnetic effect. These developments will lead to establishing an ultra-precise reference frame based on Earth and the solar system. It will be useful for fundamental astronomy and space navigation.

Astrodynamical Equation

- **Astrodynamical Equation**: *In the solar system*, the equation of motion of a celestial body or a spacecraft is given by the astrodynamical equation
- $\mathbf{a} = \mathbf{a}_N + \mathbf{a}_{1PN} + \mathbf{a}_{2PN} + \mathbf{a}_{Gal\text{-}Cosm} + \mathbf{a}_{GW} + \mathbf{a}_{non\text{-}grav}$,   (1) (Ni 2010, 2016 and refs therein)
- where **a** is the acceleration of the celestial body or spacecraft,
- $\mathbf{a}_N$ is the acceleration due to Newtonian gravity,
- $\mathbf{a}_{1PN}$ **the acceleration due to first post-Newtonian effects,**
- $\mathbf{a}_{2PN}$ the acceleration due to second post-Newtonian effects,
- $\mathbf{a}_{Gal\text{-}Cosm}$ **the acceleration due to Galactic and cosmological gravity,**
- $\mathbf{a}_{GW}$ the acceleration due to **GWs**, and
- $\mathbf{a}_{nongrav}$ the acceleration from all non-gravitational origins.
- **Distances between spacecraft depend critically on the solar-system gravity (including gravity induced by solar oscillations), underlying gravitational theory and incoming GWs.**
- **A precise measurement of these distances as a function of time will enable the cause of variation to be determined.**

ASTROD-GW & LISA

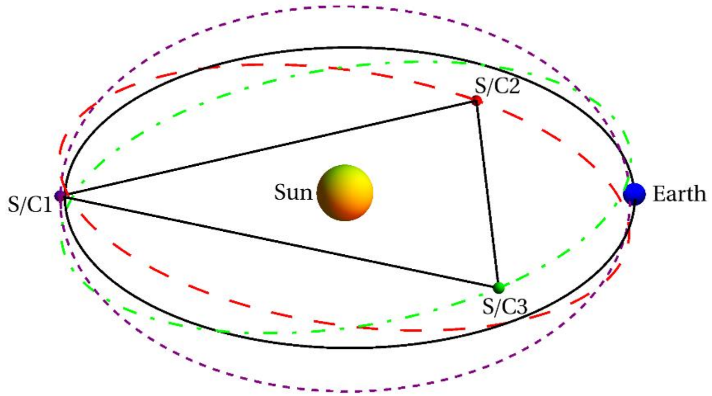

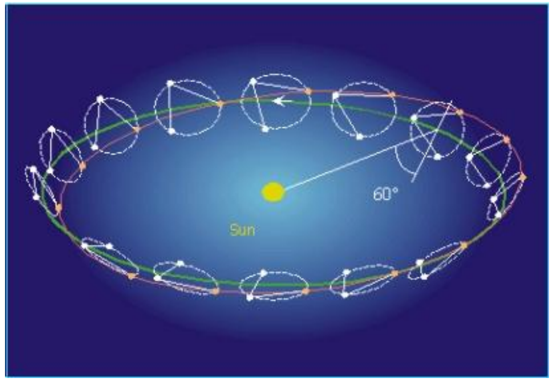

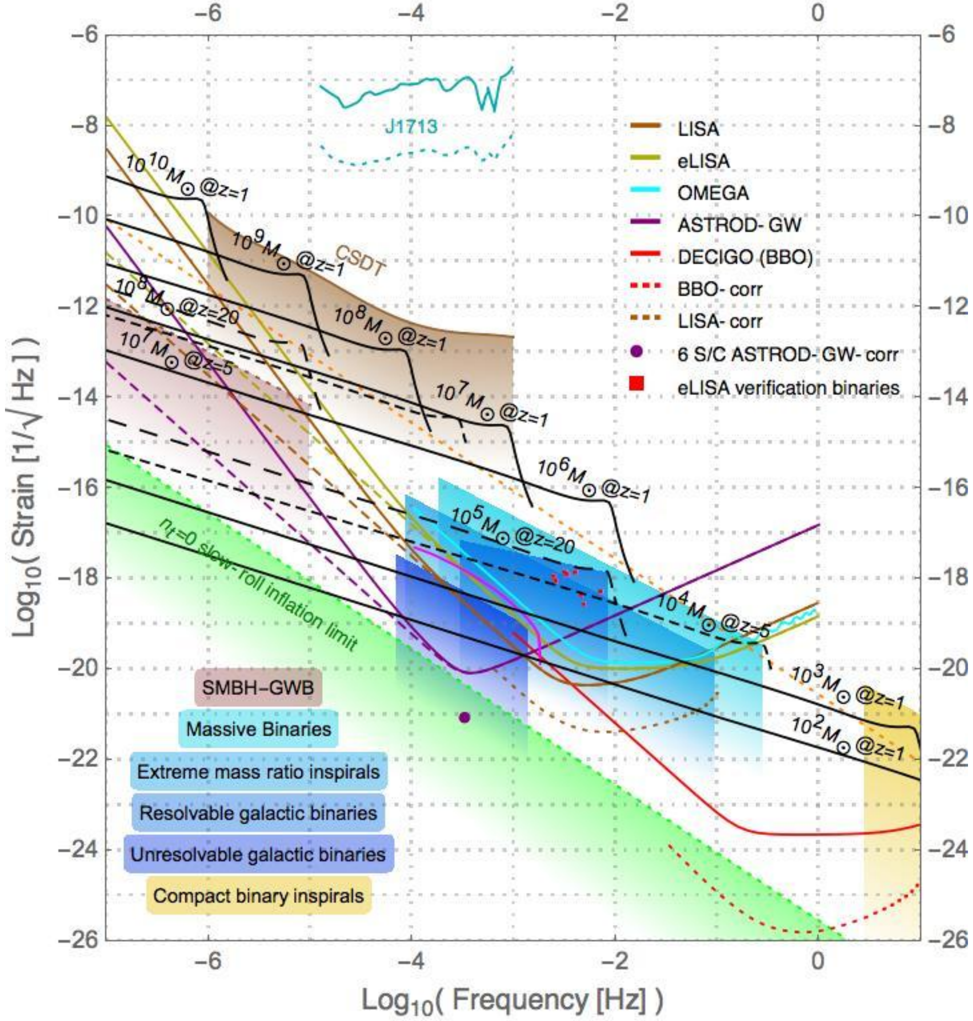

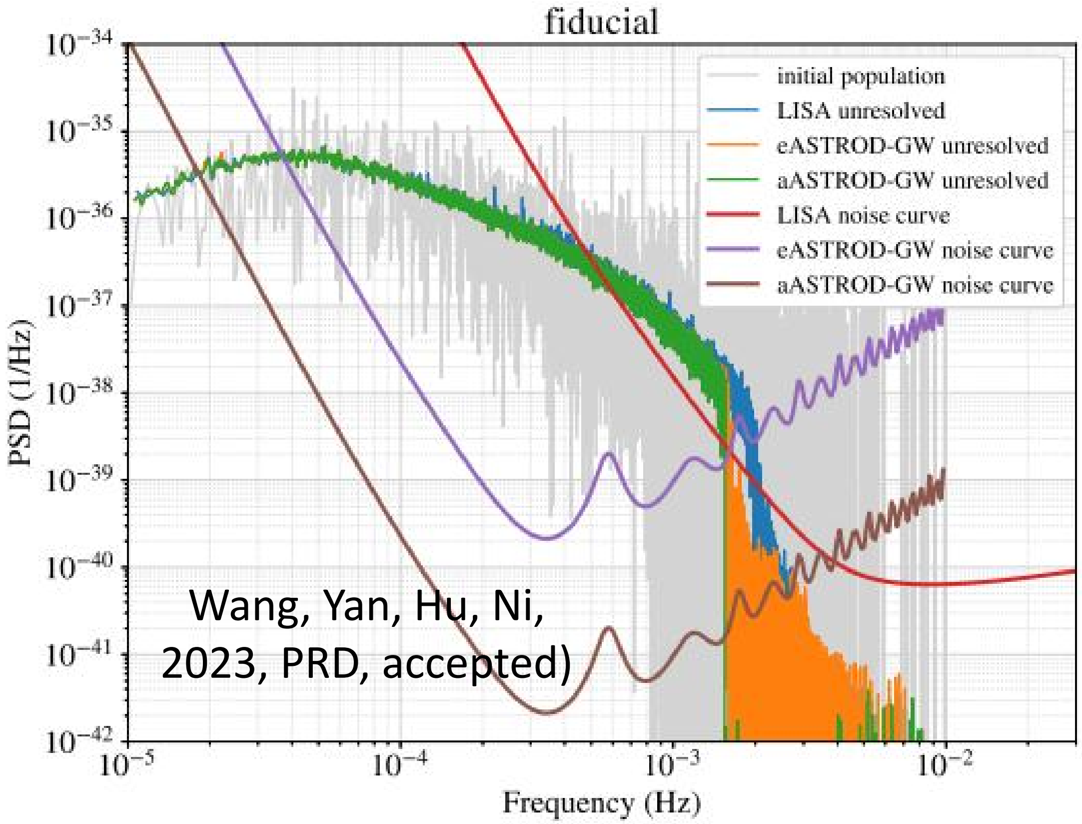

Wang, Yan, Hu, Ni,
2023, PRD, accepted)

A compilation of GW Mission Proposals

Table 1. A Compilation of GW Mission Proposals

Mission Concept	S/C Configuration	Arm length	Orbit Period	S/C #	Acceleration noise [$fm/s^2/Hz^{1/2}$]	laser metrology noise [$pm/Hz^{1/2}$]
Solar-Orbit GW Mission Proposals						
LISA[9]	Earth-like solar orbits with 20° lag	5 Gm	1 year	3	3	20
eLISA[21]	Earth-like solar orbits with 10° lag	1 Gm	1 year	3	3	12 (10)
ASTROD-GW[36-40]	Near Sun-Earth L3, L4, L5 points	260 Gm	1 year	3	3	1000
Big Bang Observer[45]	Earth-like solar orbits	0.05 Gm	1 year	12	0.03	1.4×10^{-5}
DECIGO[44]	Earth-like solar orbits	0.001 Gm	1 year	12	0.0004	2×10^{-6}
ALIA[47]	Earth-like solar orbits	0.5 Gm	1 year	3	0.3	0.6
TAIJI (ALIA-descope)[48]	Earth-like solar orbits	3 Gm	1 year	3	3	5-8
Super-ASTROD[42]	Near Sun-Jupiter L3, L4, L5 points (3 S/C), Jupiter-like solar orbit(s)(1-2 S/C)	1300 Gm	11 year	4 or 5	3	5000
Earth-Orbit GW Mission Proposals						
OMEGA[54,55]	0.6 Gm height orbit	1 Gm	53.2 days	6	3	5
gLISA/GEOGRAWI[49-51]	Geostationary orbit	0.073 Gm	24 hours	3	3, 30	0.3, 10

ASTROD-GW Orbit and Time Delay Interferometry (TDI)

(i) for the orbit of S/C I

$$\begin{pmatrix} x^{\mathrm{I}} \\ y^{\mathrm{I}} \\ z^{\mathrm{I}} \end{pmatrix} = \begin{pmatrix} a\cos\omega t - \xi a \cos\omega t \\ a \sin\omega t \\ a\cos\omega t \sin\lambda \end{pmatrix},$$

(ii) for the orbit of S/C II

$$\begin{pmatrix} x^{\mathrm{II}} \\ y^{\mathrm{II}} \\ z^{\mathrm{II}} \end{pmatrix} = \begin{pmatrix} a\left[\left(-\frac{1}{2}\right)\cos\omega t - \left(\frac{3^{1/2}}{2}\right)\sin\omega t\right] \\ \quad + \left(\frac{a}{2}\right)\xi\left[\left(\frac{3^{1/2}}{2}\right)\sin\omega t - \frac{1}{2}\cos\omega t\right] \\ a\left[\left(-\frac{1}{2}\right)\sin\omega t + \left(\frac{3^{1/2}}{2}\right)\cos\omega t\right] \\ \quad + \left(\frac{3^{1/2}}{2}\right)a\xi\left[\left(\frac{3^{1/2}}{2}\right)\sin\omega t - \frac{1}{2}\cos\omega t\right] \\ a\sin\lambda\left[\left(\frac{3^{1/2}}{2}\right)\sin\omega t - \frac{1}{2}\cos\omega t\right] \end{pmatrix},$$

(iii) for the orbit of S/C III

$$\begin{pmatrix} x^{\mathrm{III}} \\ y^{\mathrm{III}} \\ z^{\mathrm{III}} \end{pmatrix} = \begin{pmatrix} a\left[\left(-\frac{1}{2}\right)\cos\omega t + \left(\frac{3^{1/2}}{2}\right)\sin\omega t\right] \\ \quad + \left(\frac{a}{2}\right)\xi\left[\left(\frac{3^{1/2}}{2}\right)\sin\omega t - \frac{1}{2}\cos\omega t\right] \\ a\left[\left(-\frac{1}{2}\right)\sin\omega t - \left(\frac{3^{1/2}}{2}\right)\cos\omega t\right] \\ \quad - \left(\frac{3^{1/2}}{2}\right)a\xi\left[\left(-\frac{3^{1/2}}{2}\right)\sin\omega t - \frac{1}{2}\cos\omega t\right] \\ a\sin\lambda\left[\left(-\frac{3^{1/2}}{2}\right)\sin\omega t - \frac{1}{2}\cos\omega t\right] \end{pmatrix}.$$

- Sagnac TDI:

  Path 1, SC1 --> SC2 --> SC3 --> SC1

  Path 2, SC1 --> SC3 --> SC2 --> SC1

- next order Sagnac TDI

  Path 1, SC1 --> SC2 --> SC3 --> SC1

  --> SC3 --> SC2 --> SC1

  Path 2, SC1 --> SC3 --> SC2 --> SC1

  --> SC2 --> SC3 --> SC1

ASTROD-GW, Sagnac Effect and Lense-Thirring Effect

- Sagnac Effect $\Delta\varphi \approx (8\pi/\lambda c)\,\boldsymbol{\omega}\boldsymbol{A}$, $\Delta t \approx 4\,\boldsymbol{\omega}\boldsymbol{A}/c^2$.

$$\Delta t_0^{sagnac} \approx 4\,\boldsymbol{\omega}\boldsymbol{A}/c^2 = 257608.17\ \mu\text{s}, \qquad (4)$$

$\boldsymbol{\omega}$ = 2π/one sidereal year = 2π/(31558149.984 + 0.010 T) = $1.9909865788600\times10^{-7}$ Hz

with T = epoch from 1900.0 in centuries), (5)

$\boldsymbol{A}$ = area spanned by the formation = $(1/2)\cdot(3/2)\cdot3^{1/2}\cdot a^2$ = 14535.926528656 Gm^2

with a = 1 AU = 1495978700 m). (6)

- Since S/C are moving, the extra distance the light (counterclockwise) needs to travel from S/C III to S/C I is

$$(1/c^2)\cdot(d\boldsymbol{r}^{\mathrm{I}}/\mathrm{d}t)\cdot(\boldsymbol{r}^{\mathrm{I}}-\boldsymbol{r}^{\mathrm{III}}) = (3^{1/2}/2)\cdot(\omega a^2/c^2)\cdot[1-\lambda^2\cdot(1+(3^{1/2}/2)\cdot\sin(2\omega t-60°)+O(\lambda^4)]. \qquad (8)$$

Similarly, for the reverse direction

$$(1/c)\cdot(d\boldsymbol{r}^{\mathrm{III}}/\mathrm{d}t)\cdot(\boldsymbol{r}^{\mathrm{III}}-\boldsymbol{r}^{\mathrm{I}}) = -(3^{1/2}/2)\cdot(\omega a^2/c^2)\cdot[1-\lambda^2\cdot(1+\text{periodic term}+O(\lambda^4)]. \qquad (9)$$

TDI configuration time delay

- For first generation Sagnac-α, Sagnac-β and Sagnac-γ TDI configurations for ASTROD-GW of various degrees of formation inclination (0°, 0.5°, 1°, 1.5°, 2°, 2.5°, and 3°

  with respect to the ecliptic plane, we list their rms path differences in the third, fourth and fifth rows as calculated numerically for 3700 days as obtained in [Wang & Ni 2015] using CGC2 post-Newtonian ephemeris;
- the averages of these 3 TDI's differences are listed in the sixth row with numerical values of Sagnac effects calculated according to (10) listed in the seventh row, the differences of each inclined formation w.r..t. the uninclined formation in the eighth row and the estimation of the Lense-Thirring in the nine (last) row.

$$\Delta t = 3\cdot 3^{1/2}\cdot(\omega a^2/c^2)\cdot[1 - \lambda^2/2 + O(\lambda^4)] = \Delta t_0^{sagnac}\cdot[1 - \lambda^2/2 + O(\lambda^4)]$$

$$= 257608.17\ [1 - \lambda^2 + O(\lambda^4)]\ \mu s$$

Sagnac TDI configuration	ASTROD-GW TDI path difference						
	0° [μs]	0.5° [μs]	1° [μs]	1.5° [μs]	2° [μs]	2.5° [μs]	3° [μs]
Sagnac-α	257610	257590	257531	257432	257293	257115	256898
Sagnac-β	257608	257588	257529	257431	257294	257118	256902
Sagnac-γ	257607	257588	257530	257432	257297	257122	256909
average	257608.3	257588.7	257530	257431.7	257294.7	257118.3	256903
Sagnac part	257608	257588	257530	257431	257294	257.118	256902
Sagnac part due to λ ≠ 0	0	-19.62	-78.47	−176.56	−313.88	−490.44	−706.24
Lense-Thirring part	$0.263\chi\cos\lambda' \times 10^{-6}$	$0.263\chi\cos\lambda' \times 10^{-6}$	$0.263\chi\cos\lambda' \times 10^{-6}$	$0.263\chi\cos\lambda' \times 10^{-6}$	$0.263\chi\cos\lambda' \times 10^{-6}$	$0.263\chi\cos\lambda' \times 10^{-6}$	$0.263\chi\cos\lambda' \times 10^{-6}$

Lense-Thirring (Gravitomagnetic, Frame-dragging) Delay

$$\Delta t_{TT} = \int dt = (1/c)\int dz[1 + (1+\gamma)\, U + O(h^2)] = \Delta t^N + [(1+\gamma)/2]\, \Delta t_S^{GR}$$
$$= (1/c)\,(z_2 - z_1) + (1+\gamma)\,(GM_{sun}/c^3)\, ln\{[(z_2^2 + b^2)^{1/2} + z_2]/[(z_1^2 + b^2)^{1/2} + z_1]\} +$$
$$(2/c^3)\, G_N J \cos\lambda' \cdot \{2/b - 1/(z_2^2+b^2)^{1/2} - 1/(z_1^2+b^2)^{1/2}\} + O(h^2),\ (z_1 < 0,\ z_2 > 0),\ (22)$$

where the first term is the Newtonian travel time Δt^N (Römer delay), the second term is the relativistic Shapiro time delay [S1] with Δt_S^{GR} the general relativistic Shapiro time delay, the third term is the Lense-Thirring effect $\Delta t_{L\text{-}T}^{GR}$ on the travel time, b is the impact parameter of light propagation to the Sun, and λ' is the angle between the normal of the orbit plane and the solar angular momentum direction.

Ephemeris orbit of ASTROD-GW
(Wang & Ni 2015)

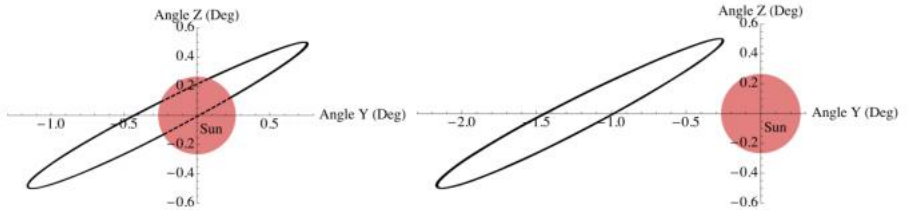

Fig. 2. S/C1 view form Earth before rotating the initial conditions by an angle (left diagram) and after rotating by an angle 2.0° (right diagram) for the case of inclination angle 1.0°.

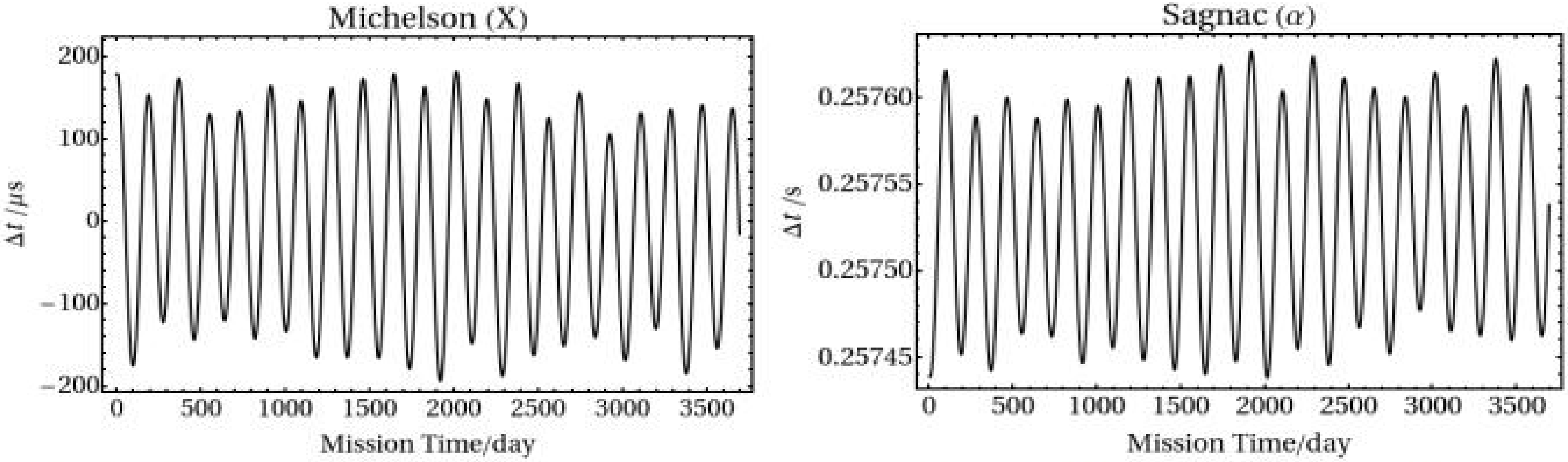

Fig. 4. Path length differences between two optical paths of the Unequal-arm Michelson TDI configuration (X) and Sagnac TDI configuration (α) for ASTROD-GW orbit formation with 1° inclination.

Second Generation Sagnac TDIs (Wang & Ni 2015)

Table 5. Compilation of the rms path length differences of various TDI configurations in the case of one interferometric detector with two arms (vertex at S/C1) for various degrees of ASTROD-GW formation inclination (0°, 0.5°, 1°, 1.5°, 2°, 2.5° and 3°) with respect to the ecliptic plane. [Nominal ASTROD-GW arm length: 260 Gm]

TDI configuration		ASTROD-GW TDI path difference ΔL						
		0°[ns]	0.5°[ns]	1°[ns]	1.5°[ns]	2.0 [ns]	2.5 [ns]	3.0 [ns]
n=1	[ab, ba]	22	41	152	342	608	951	1370
	Sagnac-α	257610 µs	257590	257531	257432	257293	257115	256898
µs	Sagnac-β	257608	257588	257529	257431	257294	257118	256902
	Sagnac-γ	257607	257588	257530	257432	257297	257122	256909

ASTROD-GW sensitivity for detection solar Lense-Thirring

- At 10^{-4} Hz, the laser metrology sensitivity is 1000 ps $Hz^{-1/2}$, the sensitivity for 10 year of detection is times $(3 \times 10^8\ s)^{-1/2}$, i.e. 0.6 ps
- This is marginal, one needs enhancement like another spacecraft ranging with the near L3 point spacecraft (100 times effect)
- With enhanced power, say 10 fold, or 3-fold increase of sensitivity
- Direct fitting the ephemeris may reach better results, this is under study
- When the ephemeris is improved 20 years later (the time to have an ASTROD-GW like mission) this would be OK, we are aiming at 0.1 % of χ.

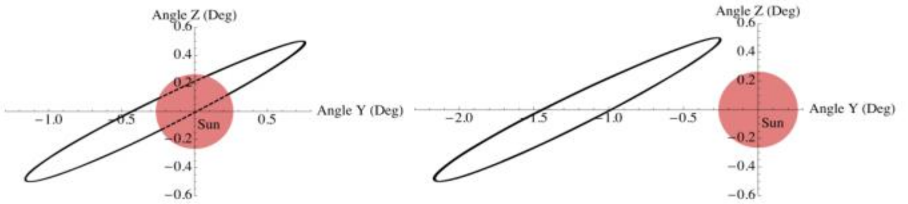

Fig. 2. S/C1 view form Earth before rotating the initial conditions by an angle (left diagram) and after rotating by an angle 2.0° (right diagram) for the case of inclination angle 1.0°.

How about Measuring Galactic Angular Momentum

- ASTROD-GW like missions have enclosed area 4 order of magnitudes larger than LISA-like missions. Super-ASTROD have 25-fold more area than ASTROD-GW. Therefore ASTROD-GW like missions and Super-ASTROD would have better chance.
- Further study needed

Gyrogravitational ratio of particles

- For gravitational interaction, we can define the gyrogravitational factor as the gravitomagnetic moment divided by angular momentum. The gyrogravitational ratio then normalizes that for ordinary angular momentum to be 1.
- What would be the gyrogravitational ratios of elementary particles? If they differ from one, they will definitely reveal some inner gravitational structures of elementary particles. These will give clues to the microscopic origin of gravity.
- GP-B verifies the frame-dragging effect on gyro to 19% accuracy. Would intrinsic spin have the same property? This could be tested by using spin-polarized bodies (e.g. polarized solid He3) instead of rotating gyros in a GP-B type experiment to measure the He3 gyrogravitational ratio (Ni 1983c).
- Atom interferometry (Berman 1997, Dimopoulos et al 2008), nuclear spin gyroscopy (Kornack et al 2005) and superfluid He3 gyrometry (Mukharsky et al 1999, Avenel et al 2004, Chui and Penanen 2005), when developed, may contribute to this very difficult task too.
- The measurement of gyrogravitational ratio of elementary particles would probe the microscopic origin of gravity. More specifically, it would probe the following things: (i) WEP II for polarized bodies; (ii) torsion coupling; (iii) metric-affine connection theory of gravity; (iv) Yang's approach to gravity; (v) 'The origin of equivalence is identity' conjecture; (vi) microscopic theories to come in the future.

Co-magnetometer and Earth rotation Measurement

PHYSICAL REVIEW LETTERS **130**, 201401 (2023)

Editors' Suggestion | Featured in Physics

Search for Spin-Dependent Gravitational Interactions at Earth Range

S.-B. Zhang,[1] Z.-L. Ba,[1] D.-H. Ning,[1] N.-F. Zhai,[2] Z.-T. Lu,[1,3,*] and D. Sheng[2,3,†]

[1]*CAS Center for Excellence in Quantum Information and Quantum Physics, School of Physical Sciences, University of Science and Technology of China, Hefei 230026, China*

[2]*Department of Precision Machinery and Precision Instrumentation, Key Laboratory of Precision Scientific Instrumentation of Anhui Higher Education Institutes, University of Science and Technology of China, Hefei 230027, China*

[3]*Hefei National Laboratory, University of Science and Technology of China, Hefei 230088, China*

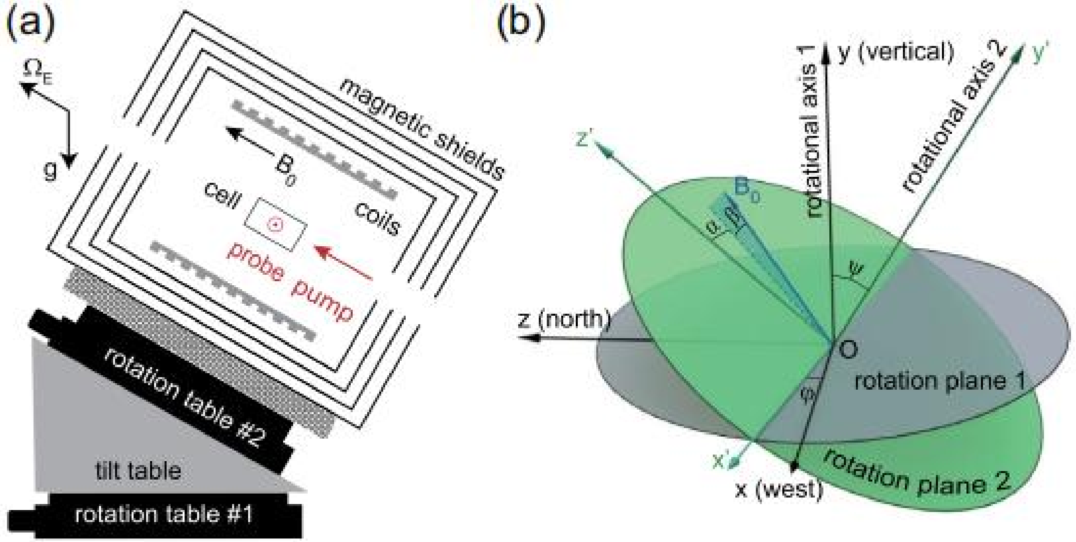

By measuring the ratio of nuclear spin precession frequencies between 129Xe and 131Xe as the bias field is flipped between being parallel and antiparallel to the Earth rotation direction, **they determine the Earth rotation rate with an accuracy of 2.6 nHz (1σ).**

Great advance in sensitivity during last 2 years

- (i) co-magnetometer method: **2.6 nHz accuracy**
- (ii) AI method: 0.04 ppm when considering the 1000 : 1 signal-to-noise level per shot with TR=400ms and δf=10 kHz. It is expected that the uncertainty of the Earth rotation measurement reaches 10^{-8} order.
- (iii) passive ring laser gyro: 400 pHz@10000 s resolution
- (iv) active ring laser gyro: Feasible to reach 1 part in 10^{11} of Ω_E

Referece Frames

- ICRS International Celestial Reference System
    - Optical
    - Dynamical
- ITRS International Terrestrial Reference System
    - Polar motion
    - Earth Rotation

Matching of ICRS and ITRS

Ephemerides, LLR

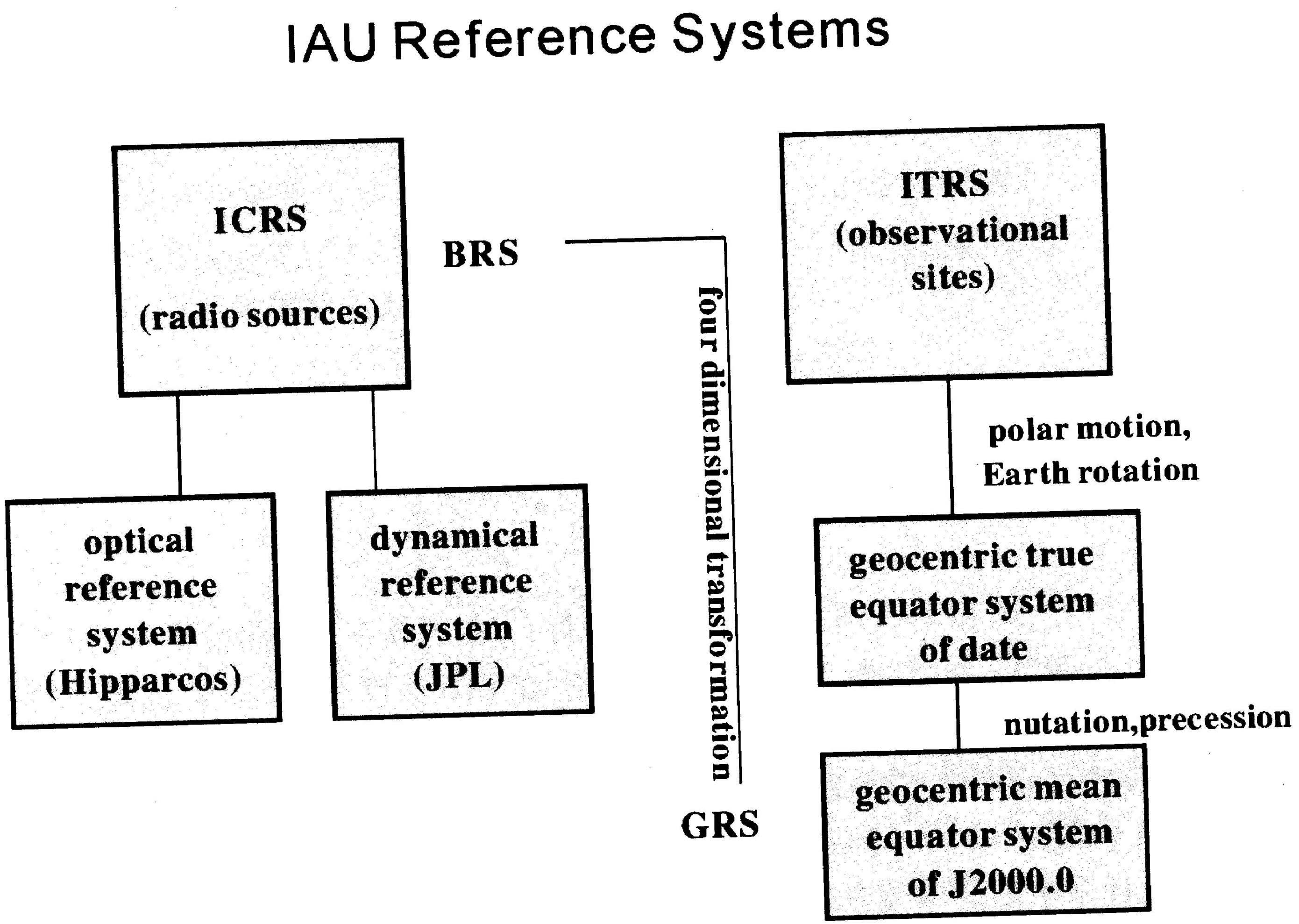

IAU time scale

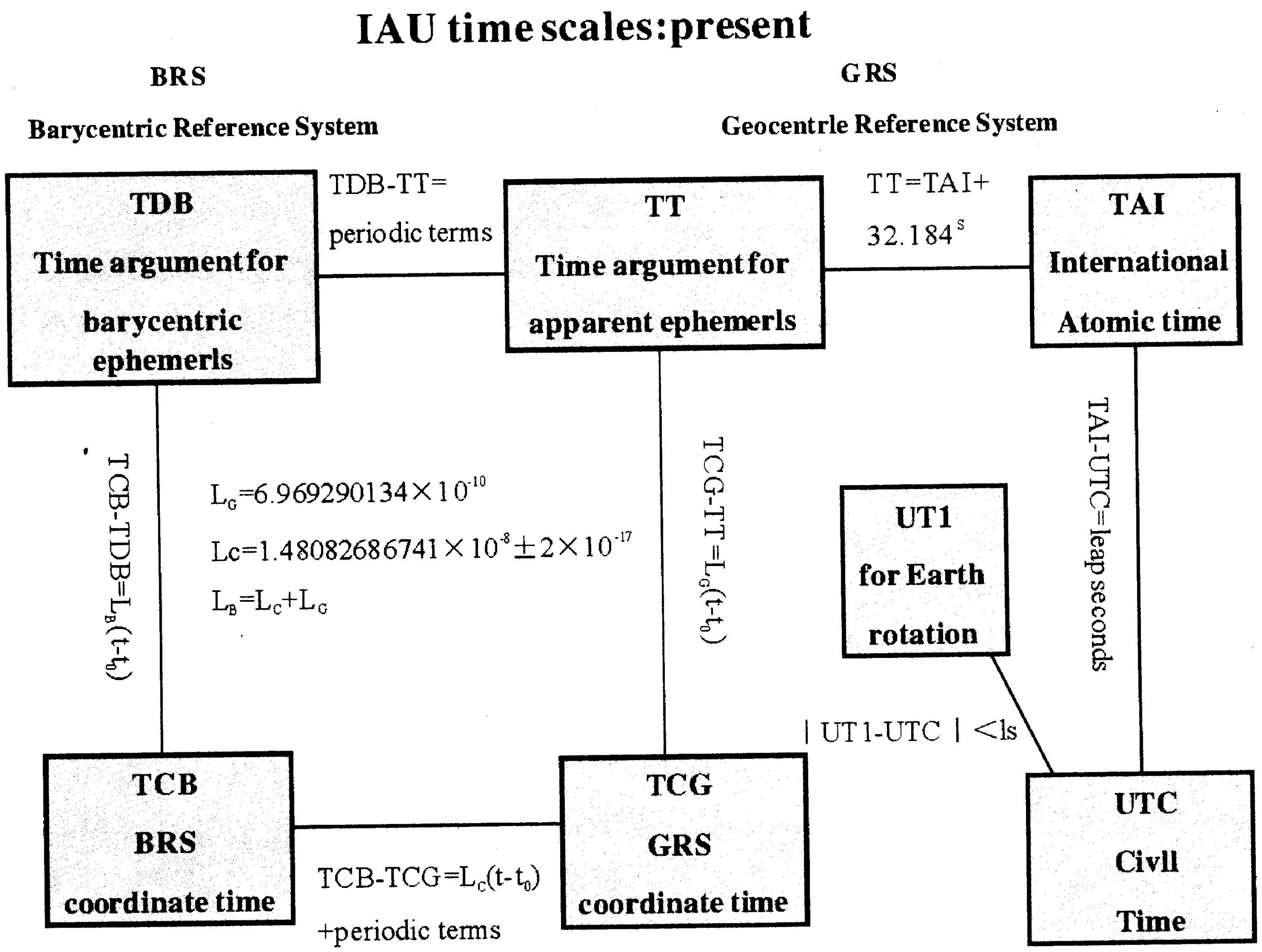

Let us look forward to the coming Workshops in Hefei 2025 (& Germany 2027)

We are here now in 2023